Helical Structures

International Edition: DOI: 10.1002/anie.201606833
German Edition: DOI: 10.1002/ange.201606833

Crosslinked Aspartic Acids as Helix-Nucleating Templates

Hui Zhao[+], Qi-Song Liu[+], Hao Geng[+], Yuan Tian, Min Cheng, Yan-Hong Jiang, Ming-Sheng Xie, Xiao-Gang Niu, Fan Jiang, Ya-Ou Zhang, Yuan-Zhi Lao, Yun-Dong Wu, Nai-Han Xu,* and Zi-Gang Li**

Abstract: *Described is a facile helix-nucleating template based on a tethered aspartic acid at the N-terminus [terminal aspartic acid (TD)]. The nucleating effect of the template is subtly influenced by the substituent at the end of the side-chain-end tether as indicated by circular dichroism, nuclear magnetic resonance, and molecular dynamics simulations. Unlike most nucleating strategies, the N-terminal amine is preserved, thus enabling further modification. Peptidomimetic estrogen receptor modulators (PERMs) constructed using this strategy show improved therapeutic properties. The current strategy can be regarded as a good complement to existing helix-stabilizing methods.*

Protein–protein interactions (PPIs) with either large or shallow interfaces are generally intractable for small-molecule modulators, but easily targetable by peptide epitope mimics.[1] Many PPIs involved in vital biological processes are mediated by helices.[2] However, short helices did not become promising therapeutics until the seminal work by Verdine and others who applied crosslinking[3] and nucleation[4] strategies to constrain peptides in a helical conformation.[1a] The conformation constraints lead to improved peptide stability and cell permeability, thereby making intracellular targets potentially accessible by originally fragile and hydrophilic peptides.

The nucleation strategy may maximize recognition specificity of the original sequence without compromising the molecular recognition surface.[5] The most successful helix nucleation strategy, namely the hydrogen-bond surrogate (HBS) system,[4d,6] features the replacement of a hydrogen bond at the N-terminus by a covalent link.[7] Among different types of HBS systems, alkene-tethered HBS helices have been applied to various biologically relevant targets.[8] Besides HBSs, other nucleating templates generally provide hydrogen-bond donors to mimic the first turn of a helix.[4a–c,9]

Construction of the alkene-linked HBS helices usually requires microwave-assisted reactions.[10] Other helix-nucleating templates with rigid carbonyl mimics[4a–c,9] require multistep syntheses and bulky appendages, which limit further applications.[5] No nucleating template constructed by a simple side-chain-end crosslinking has been documented. Herein, we report a facile helix-nucleating template based on a tethered aspartic acid at the N-terminus (Scheme 1).

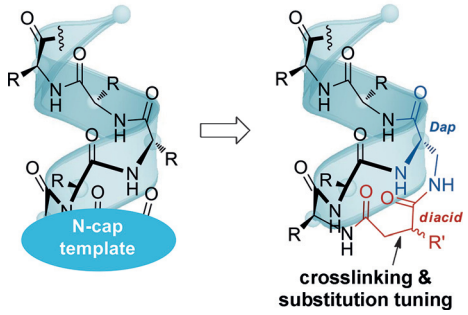

Scheme 1. Development of crosslinked diacids as N-cap nucleating templates.

Amino acids with additional hydrogen-bonding capabilities such as aspartic acid or asparagine are frequently found at the N-terminus of helices.[11] Thus, we decided to use an amide bond, which has a hydrogen-bond donor and an acceptor, to construct a linkage at the end of the side chain. Based on the tether length of the HBS,[4d] we started with 2,3-diaminopropionic acid (Dap)[12] and succinic acid to yield a six-membered crosslink. We synthesized a linear pentapeptide (**1**) and a cyclic counterpart (**2**), and initially investigated their conformation by circular dichroism (CD) spectroscopy (Figure 1). Although the cyclic peptide **2** shows enhanced helicity compared to the linear peptide **1**, as shown in Figure 1 and Table S1, the helicity of **2** is low to moderate according to

[*] Dr. H. Zhao,[+] Dr. Q. S. Liu,[+] Dr. H. Geng,[+] Dr. Y. Tian, Dr. Y. H. Jiang, Dr. M. S. Xie, Dr. F. Jiang, Prof. Dr. Y. D. Wu, Prof. Dr. Z. G. Li
School of Chemical Biology and Biotechnology
Shenzhen Graduate School of Peking University
Shenzhen, 518055 (China)
E-mail: wuyd@pkusz.edu.cn
lizg@pkusz.edu.cn

Dr. Q. S. Liu[+]
Shenzhen Key Lab of Tissue Engineering
The Second People's Hospital of Shenzhen
Shenzhen, 518035 (China)

Dr. M. Cheng, Prof. Dr. Y. O. Zhang, Prof. Dr. N. H. Xu
Key Lab in Healthy Science and Technology
Division of Life Science, Shenzhen Graduate School of Tsinghua University, Shenzhen, 518055 (China)
E-mail: xu.naihan@sz.tsinghua.edu.cn

Dr. X. G. Niu
College of Chemistry and Molecular Engineering
Beijing Nuclear Magnetic Resonance Center
Peking University, Beijing, 100871 (China)

Dr. Y. Z. Lao
School of Pharmacy, Shanghai University of Traditional Chinese Medicine, Shanghai, 201203 (China)

[+] These authors contributed equally to this work.

Supporting information for this article can be found under: http://dx.doi.org/10.1002/anie.201606833.

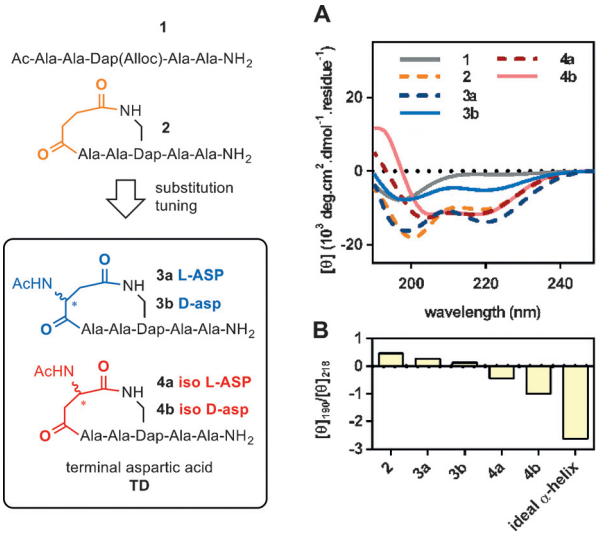

Figure 1. Helix stabilization by terminal $i,i+3$ tethered diacids. A) CD spectra of **1**, **2**, **3a**, **3b**, **4a**, **4b**. All CD spectral measurements were performed in PBS buffer, 10 mM, pH 7.4, 298 K, concentration normalized. Dap: 2,3-diaminopropionic acid. B) $[\theta]_{190}/[\theta]_{218}$ for **2**, **3a**, **3b**, **4a**, and **4b**.

the CD data. We attributed this limited helix-inducing ability to an unfavorable conformation of the tether.

The peptide conformation can be affected by the configuration of atoms not only within but also outside of the peptide backbone.[13] Therefore, we hypothesized that cyclic peptides tethered by diacids of different substitution types might provide a library for an optimal nucleating template. We accordingly synthesized the four cyclic peptides **3a**, **3b**, **4a**, and **4b** using L- and D-aspartic acid, with different linking directions of the aspartic acid (Figure 1; the **a** and **b** refer to the L and D isomers, respectively). Based on the enhanced $[\theta]_{218}$ in Figure 1 A and the $[\theta]_{190}/[\theta]_{218}$ ratio in Figure 1 B, **3a**, **4a**, and **4b** have increased helicity (see Table S1 in the Supporting Information), while **3b** shows a decrease in helicity compared to **2**. Thus, the crosslinked aspartic acid at the N-terminus might be used as an N-cap template to nucleate helices.

For a detailed analysis of the peptide structure, we characterized **3a**, **4a**, and **4b** by two-dimensional NMR spectroscopy (10% D_2O/PBS). For these peptides, low coupling constants ($^3J_{NHCH\alpha} < 6$ Hz; see Table S2) for amide resonances and long-range ROEs (Figure 2 A) suggest that **4b** presents a better helix than both **3a** and **4a.**[3b] Notably, the first Ala (from N-terminus to C-terminus) exhibits a small $^3J_{NHCH\alpha}$ coupling constant (3.5 Hz for **3a**, 3.0 Hz for **4a**, and 2.0 Hz for **4b**),[14] thus suggesting a smaller Phi angle than an ideal α-helical conformation (3.9 Hz).[15] In contrast, larger $^3J_{NHCH\alpha}$ coupling constants in the remaining residues (most between 4.0 and 6.0 Hz except for Dap in **4a** (6.4 Hz; see Table S2) indicate a loose helical structure, which might explain the low $[\theta]_{190}/[\theta]_{218}$ ratio in the CD spectra. Comparatively, **4a** and **4b** show stronger $i,i+1$ ROEs than **3a** (Figure 2 A; see Table S2). Meanwhile, **4b** shows more long-range ROEs than **3a** and **4a**. Both observations were consistent with their $[\theta]_{190}/[\theta]_{218}$ ratio ranking (Figure 1 B).

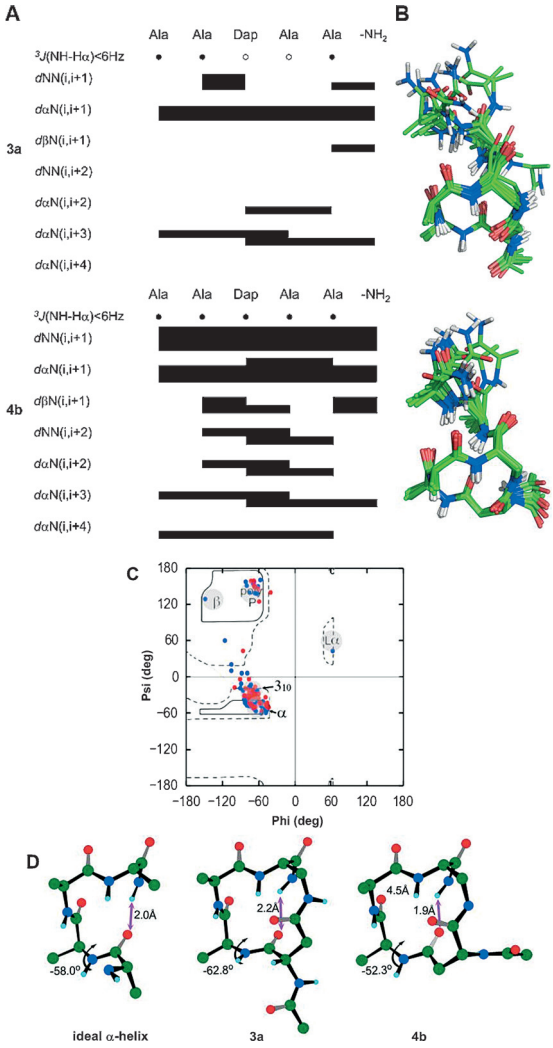

Figure 2. A) ROE summary diagram of **3a** and **4b**. (10% D_2O/PBS) ROEs concerning the terminal aspartic acid were omitted for clarity. Two $^3J_{NHCH\alpha}$ coupling constants were not determined because of signal overlap. B) Ten lowest-free-energy solution structures calculated for **3a** and **4b**. C) Ramachandran plots of (ϕ, ψ) angles derived from the average of the ten lowest-energy solution structures calculated for **3a** (blue) and **4b** (red). D) Representative structures of **3a** and **4b**. Double-ended arrows indicate α-helical hydrogen bonds.

Generally, **3a**, **4a**, and **4b** show a flexible helix with local nonhelical features and **4b** presents a better helix than both **3a** and **4a.**

To better understand the structural effect of the linkers, we carried out replica-exchange molecular dynamics (REMD) simulations on **3a** and **4b**, chosen for their representative $^3J_{NHCH\alpha}$ coupling constants of Ala2 (3.5 and 2.0 Hz,respectively; Figure 2 B). Our recently developed residue-specific force field[16] RSFF2[17] was used to treat each peptide except for the non-natural side chain, which was described by the generalized Amber force field (GAFF)[18] with restrained electrostatic potential (RESP)[19] charges. The RSFF2 has shown advantages in studying cyclic peptides.[20] For accurate description of the non-natural linkage amino acids, three ϕ angle restraints (see Table S3) on the rings were

used to avoid $^3J_{NHC\alpha}$ violations. Converged conformational sampling was achieved for each peptide. All calculated $^3J_{NHC\alpha}$ couplings and NOEs from simulated structures sampled at 300 K are in good agreement with experimental data of these cyclic peptides (see Table S4 and Figure S1). Further, clustering analysis was performed on the simulated structures, using the "gromos"[21] method with a 0.5 Å cutoff of the backbone and Cβ RMSD. According to the 10 lowest-free-energy structures in Figure 2B, the macrocycles of **3a** and **4b** are rather rigid. Moreover, in agreement with the observations in CD spectra (Figure 1), **3a** shows a more fraying C-terminus than **4b** (Figure 2B), thus suggesting its lower helix-inducing effect. This data is also supported by RMSD, as well as Ramachandran (ϕ, ψ) plots obtained from the peptide structures (Figure 2C).

For a detailed comparison, Figure 2D shows representative structures (centroid of the largest cluster) of the ring of **3a** and **4b** from REMD simulations. The rises along the helix axis of the first three units (calculated from Cα of D1 to Cα of X4) for **3a** and **4b** are 4.3 and 4.5 Å, respectively (see Table S5), and are slightly smaller than the corresponding rise of an ideal α-helix (4.6 Å). In particular, **3a** is more flat than both **4b** and ideal α-helical structures, and is in agreement with our observation that **3a** induce less helicity compared with **4b**. Furthermore, the smaller ϕ angle for Ala2 in **4b** (−52.3°) than in **3a** (−62.8°) makes the carbonyl group next to the N-terminus more favorable for forming α-helical hydrogen bond (Figure 2D). In conclusion, the substitution pattern might affect the subtle conformational changes of the macrocycles and, further, the helix-nucleating effects.

We then focused on **4b** and investigated the effect of other factors on the enhanced helicity of the terminal iso D-aspartic acid strategy. When the N-terminal acetyl group is removed (peptide **5**), the molar ellipticity ($[\theta]_{218}$) is reduced (Figure 3A; see Table S6). Expansion of the ring size by one atom shows a detrimental effect on the helicity as shown by the CD spectrum of peptide **6** (Figure 3A; see Table S6). The results suggested that the ring size of the macrocycle was critical for nucleation, and is similar to the case of the HBS.[22]

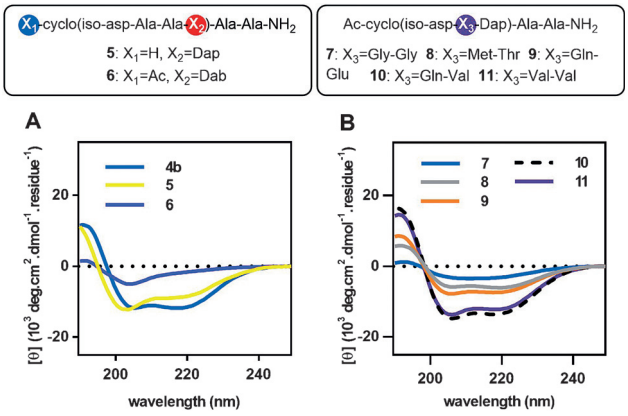

Figure 3. Peptides stabilized by terminal tethered iso D-aspartic acid. A) CD spectra of **5** and **6**. B) CD spectra of **7**–**11**. All CD spectral measurements were performed in PBS buffer, 10 mM, pH 7.4, 298 K, concentration normalized.

To confirm the helix-nucleating ability of terminal tethered iso D-aspartic acid, we also synthesized short peptides with various sequences (**7**–**11**; Figure 3B). The system showed excellent sequence tolerance for pentapeptides bearing different residues according to the CD spectra (**8**–**11**; Figure 3B; Table S6). Interestingly, Gly-containing peptides (**7**) stabilized by terminal tethered iso D-aspartic acid tend to form a helix over a random coil[3b] according to CD spectrum and low coupling constants ($^3J_{NHC\alpha} < 6$ Hz) of amide resonances (see Table S7). Notably, $d\alpha N(i,i+4)$s are observed only for **8** and **11** (see Table S7), and suggests that the transition between the 3_{10} helix and α-helix of a peptide is sequence-dependent. The large $^3J_{NHC\alpha}$ values [Thr (6.5) in **8**, see Table S7] and fewer long range ROEs of **8** and **9** (see Table S7) might explain the lower $[\theta]_{218}$ of **8** and **9** compared to that of **10** and **11** in the CD spectra (Figure 3B). Collectively, these results confirmed that the terminal tethered iso D-aspartic acid system is applicable for inducing and stabilizing helical conformations of short peptides.

After establishing the method using pentapeptides, we turned to validating the application of the terminal iso aspartic acid (TD) linking strategy for proof-of-concept development of PPI inhibitors. The estrogen receptor α (ER-α)[23] was chosen as the target. For helical modulators[24] of the ER–coactivator interaction, precise length control is necessary for efficient inhibition.[24h] Accordingly, we chose the suitably sized **PERM-2** [H-Arg-cyclo(D-cys-Ile-Leu-Cys)-Arg-Leu-Leu-Gln-NH_2],[24b] reported by Burris et al., as the model peptide. In our model, the N-terminal Arg was employed as an extra N-modification rather than an elongation. Notably, this additional site generated with the TD strategy, which can be used for further modifications,[3g] is absent in the classic helix nucleation strategy.[4d]

We initially analyzed the helix-stabilizing effect of the new strategy on long peptides. Surprisingly, in contrast with the case of pentapeptides, **12a** (terminal tethered iso L-aspartic acid) shows higher helical content than **12b** (terminal tethered iso D-aspartic acid; Figure 4A; see Table S8), thus suggesting that the relative nucleating effect was associated with either the peptide length or sequence. Further, similar to the case of **4b**, the acetylated form of **12a** [**12a Ac;** Ac-Arg-cyclo(iso-Asp-Ile-Leu-Dap)-Arg-Leu-Leu-Gln-NH_2] is more helical than **12a** (see Figure S2 and Table S8). To sum up, these results indicated that terminal iso aspartic acid (TD) templates can be used to stabilize longer peptides in water.

Furthermore, $\mathbf{12a}_{FITC}$ and $\mathbf{12b}_{FITC}$ (FITC-labelled **12a** and **12b**) exhibit excellent in vitro serum stability[25] compared to that of the linear analogue $\mathbf{13}_{FITC}$ (Figure 4B). Notably, FITC was attached to the reserved NH_2 on the tether and the additional lysine required in the HBS for fluorophore modification was avoided. The stability might be attributed to the incorporation of Dap, unnatural connection of aspartic acid, and the fixed conformation rendered by the cyclization.

The binding affinity of stabilized peptides was evaluated (Figure 4C; see Table S9). $\mathbf{12a}_{FITC}$ (85 ± 17 nM) shows a tighter binding[26] than $\mathbf{12b}_{FITC}$ (130 ± 18 nM), and might be explained by the improved positioning of the terminal amino group on the ring of $\mathbf{12a}_{FITC}$ compared to that of $\mathbf{12b}_{FITC}$. In addition, $\mathbf{12a}_{FITC}$ shows slightly higher ER subtype selectivity

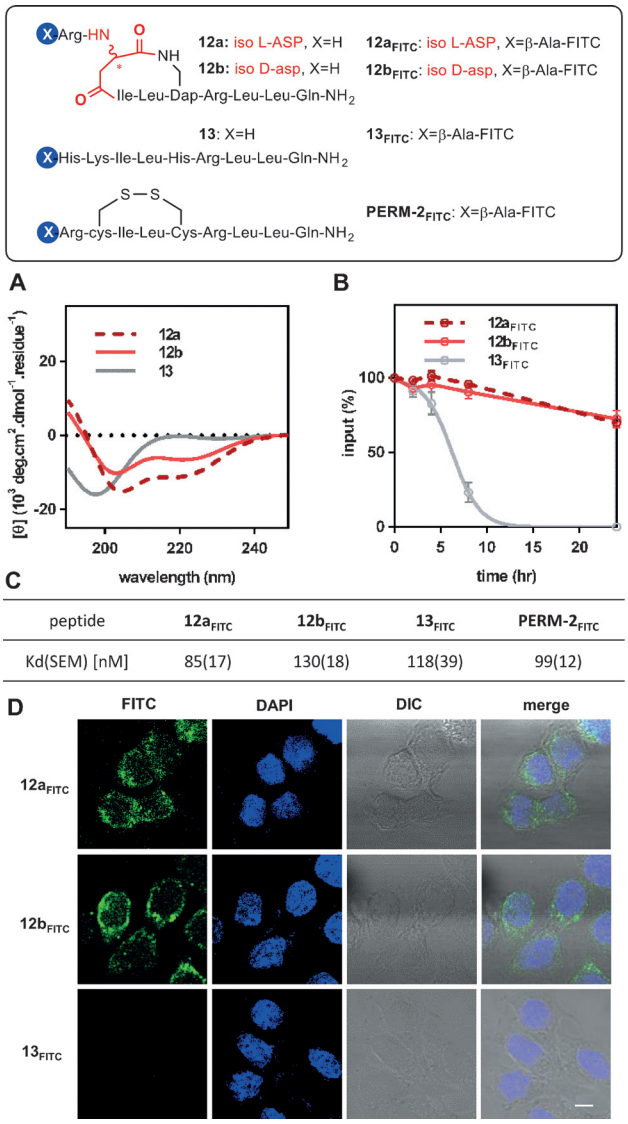

Figure 4. Improved therapeutic properties of PERMs stabilized by terminal iso aspartic acid strategy. A) CD spectra of **12a**, **12b**, and **13** (PBS, 10 mM, pH 7.4, 298 K, concentration normalized). B) Ex vivo serum stability of $\mathbf{12a}_{FITC}$, $\mathbf{12b}_{FITC}$, and $\mathbf{13}_{FITC}$. Error bars represent the standard error of mean (SEM) from more than two experiments. C) Binding affinity of $\mathbf{12a}_{FITC}$, $\mathbf{12b}_{FITC}$, $\mathbf{13}_{FITC}$, and $\mathbf{PERM\text{-}2}_{FITC}$ to ER-α. Standard error of mean (SEM) came from more than two independent experiments. D) Fluorescent confocal microscopy images of T47D cells incubated with $\mathbf{12a}_{FITC}$, $\mathbf{12b}_{FITC}$, and $\mathbf{13}_{FITC}$ (10 μM) at 310 K for 12 h. Scale bar: 5 μm.

(ER-β/ER-α = 3.2) compared to the linear analogues $\mathbf{13}_{FITC}$ (118 ± 39 nM, 1.8) and $\mathbf{14}_{FITC}$ (FITC-β-Ala-LTERH-KILHRLLQEGSPSD-NH_2, 107 ± 34 nM, 1.5), and the positive control $\mathbf{PERM\text{-}2}_{FITC}$ (99 ± 12 nM, 1.9; see Table S9). $\mathbf{12a}_{FITC}$ also shows moderate affinity (≈200 nM) to a vitamin D receptor (VDR) as shown in Table S9, and could be explained by the fact that LXXLL motif is shared by VDR coactivators.[27]

To investigate whether our stabilizing method could affect the cell permeability, we incubated T47D cells with FITC-labelled peptides (cyclic peptides $\mathbf{12a}_{FITC}$ and $\mathbf{12b}_{FITC}$, linear peptide $\mathbf{13}_{FITC}$).[25] Efficient cellular uptake is observed only for stabilized peptides (Figure 4D). $\mathbf{12a}_{FITC}$ and $\mathbf{12b}_{FITC}$ show more than twofold cellular uptake than that of $\mathbf{13}_{FITC}$ according to fluorescence activated cell sorting (FACS) results (see Figure S3). Partial decrease in cellular uptake upon addition of sodium azide and deoxyglucose suggested a mixed mechanism of cell membrane penetration. Further, co-localization of the stabilized peptides with ER-α was assessed by antibody staining and then analyzed[28] (see Figure S4). The Pearson correlation coefficient (PCC) and Manders overlap coefficient (MOC) for $\mathbf{12a}_{FITC}$ are between 0.1 and 0.2 (see Figure S5), thus suggesting that 10–20% $\mathbf{12a}_{FITC}$ co-localized with ER-α. We thought the limited penetration and nuclear accumulation of $\mathbf{12a}_{FITC}$ might account for its weak co-localization with ER-α, and could be further improved with attachment of a nuclear-targeting peptide as shown by the results of a reported positive control $\mathbf{14\text{-}R_9}_{FITC}$ (FITC-β-Ala-LTERHKILHRLLQEGSPSD-R_9-NH_2,[29] PCC ≈ 0.3, M_1 ≈ 0.15, M_2 ≈ 0.6) in Figure S5.

To verify whether our stabilized peptides bind ER-α in cells, inhibition of ER-α gene transactivation was examined through quantitative polymerase-chain reaction (qPCR) analysis[29a,30] and a luciferase reporter assay[29a] (Figure 5).

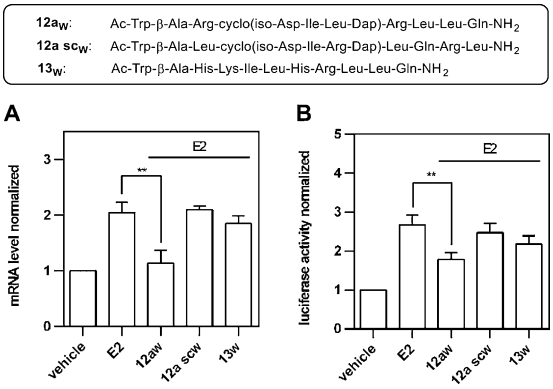

Figure 5. Cellular activities of PERMs stabilized by the TD strategy. A) Expression levels of endogenous ER mediated pS2 genes in treated T47D cells. (normalized to the mRNA levels of β-actin) B) Luciferase activities controlled by estrogen receptor element in treated 293T cells. Luciferase activities are presented as the ratio of a Firefly luciferase signal to a Renilla luciferase signal and then are normalized to the activity found in cells without treatment. Error bars represent the standard error of mean (SEM) from more than two independent experiments. $^{**}p < 0.01$.

We first evaluated the toxic effect of the peptides on cells using MTT assays (see Figure S6). Peptides show no obvious toxicity at concentrations below 40 μM on T47D or 293T cells. As with transactivation quantification, $\mathbf{12a}_{W}$ (Trp-labeled peptides are named followed by a W) induces deceased ER-α gene transactivation as indicated by the decreased pS2 mRNA levels and luminescence, while the scrambled sequence $\mathbf{12a\ sc}_{W}$ (sc represents scrambled) and linear analogue $\mathbf{13}_{W}$ have either no or a weak effect on them (Figure 5). The results indicated that cellular activities of peptides were sequence specific (LXXLL box) and cell-penetration relevant. To exclude toxicity effects that could

influence the mRNA level, we chose another housekeeping gene (β-tubulin) for normalization (see Figure S7). Consistency between two normalized results suggested the robustness of our results. Taken together, these results verified that the ER-α was the cellular target of our stabilized peptides.

In conclusion, we have developed a facile helix nucleating template based on crosslinked commercially available amino-acids-aspartic acids (TD). The nucleating effect of the template is subtly influenced by the tether structure as shown by circular dichroism, nuclear magnetic resonance spectroscopy, and molecular dynamics simulation results. Unlike most nucleating strategies, the N-terminus NH_2 is preserved, thus enabling further modification. PERMs modified with this strategy show excellent stability in serum, cell penetration, and cellular activity. These results show that this strategy may be used for development of biologically relevant helices. The method can thus be regarded as a good complement to current helix stabilizing methods.

Acknowledgments

This work is supported by the National Natural Science Foundation of China (Grant 21102007, 21372023, and 81572198), the Ministry of Science and Technology of the People's Republic of China 2015DFA31590, the Shenzhen Science and Technology Innovation Committee (SW201110018, SGLH20120928095602764, ZDSY20130331145112855, JSGG20140519105550503, and KQTD201103). We thank Dr. Lele Zhang, Dr. Hao Xie, and Dr. Liyan Zhou (the Instrument Center of the School of Chemical Biology & Biotechnology in Peking University Shenzhen Graduate School) for HRMS data collection. NMR experiments were performed at the Beijing NMR Center and the NMR facility of National Center for Protein Sciences at Peking University. We thank Prof. Olaf Wiest for helpful discussions.

Keywords: amino acids · circular dichroism · helical structures · peptides · protein–protein interactions

How to cite: *Angew. Chem. Int. Ed.* **2016**, *55*, 12088–12093
Angew. Chem. **2016**, *128*, 12267–12272

[1] a) V. Azzarito, K. Long, N. S. Murphy, A. J. Wilson, *Nat. Chem.* **2013**, *5*, 161–173; b) L. G. Milroy, T. N. Grossmann, S. Hennig, L. Brunsveld, C. Ottmann, *Chem. Rev.* **2014**, *114*, 4695–4748; c) T. A. Hill, N. E. Shepherd, F. Diness, D. P. Fairlie, *Angew. Chem. Int. Ed.* **2014**, *53*, 13020–13041; *Angew. Chem.* **2014**, *126*, 13234–13257; d) M. Pelay-Gimeno, A. Glas, O. Koch, T. N. Grossmann, *Angew. Chem. Int. Ed.* **2015**, *54*, 8896–8927; *Angew. Chem.* **2015**, *127*, 9022–9054.

[2] B. N. Bullock, A. L. Jochim, P. S. Arora, *J. Am. Chem. Soc.* **2011**, *133*, 14220–14223.

[3] a) C. E. Schafmeister, J. Po, G. L. Verdine, *J. Am. Chem. Soc.* **2000**, *122*, 5891–5892; b) N. E. Shepherd, H. N. Hoang, G. Abbenante, D. P. Fairlie, *J. Am. Chem. Soc.* **2005**, *127*, 2974–2983; c) A. Muppidi, Z. Wang, X. Li, J. Chen, Q. Lin, *Chem. Commun.* **2011**, *47*, 9396–9398; d) S. A. Kawamoto, A. Coleska, X. Ran, H. Yi, C. Y. Yang, S. Wang, *J. Med. Chem.* **2012**, *55*, 1137–1146; e) H. Jo, N. Meinhardt, Y. Wu, S. Kulkarni, X. Hu, K. E. Low, P. L. Davies, W. F. DeGrado, D. C. Greenbaum, *J. Am. Chem. Soc.* **2012**, *134*, 17704–17713; f) A. M. Spokoyny, Y. Zou, J. J. Ling, H. Yu, Y.-S. Lin, B. L. Pentelute, *J. Am. Chem. Soc.* **2013**, *135*, 5946–5949; g) Y. H. Lau, P. de Andrade, S.-T. Quah, M. Rossmann, L. Laraia, N. Skold, T. J. Sum, P. J. E. Rowling, T. L. Joseph, C. Verma, M. Hyvonen, L. S. Itzhaki, A. R. Venkitaraman, C. J. Brown, D. P. Lane, D. R. Spring, *Chem. Sci.* **2014**, *5*, 1804–1809.

[4] a) D. S. Kemp, T. P. Curran, W. M. Davis, J. G. Boyd, C. Muendel, *J. Org. Chem.* **1991**, *56*, 6672–6682; b) K. Muller, D. Obrecht, A. Knierzinger, C. Stankovic, C. Spiegler, W. Bannwarth, A. Trzeciak, G. Englert, A. M. Labhard, P. Schonholzer in *Perspectives in Medicinal Chemistry* (Eds.: B. Testa, E. Kyburz), Verlag Helvetica Chimica Acta, Basel, **1993**, pp. 513–533; c) R. E. Austin, R. A. Maplestone, A. M. Sefler, K. Liu, W. N. Hruzewicz, C. W. Liu, H. S. Cho, D. E. Wemmer, P. A. Bartlett, *J. Am. Chem. Soc.* **1997**, *119*, 6461–6472; d) R. N. Chapman, G. Dimartino, P. S. Arora, *J. Am. Chem. Soc.* **2004**, *126*, 12252–12253.

[5] A. B. Mahon, P. S. Arora, *Drug Discovery Today* **2012**, *9*, e57–e62.

[6] a) A. Patgiri, A. L. Jochim, P. S. Arora, *Acc. Chem. Res.* **2008**, *41*, 1289–1300; b) S. E. Miller, N. R. Kallenbach, P. S. Arora, *Tetrahedron* **2012**, *68*, 4434–4437; c) A. B. Mahon, P. S. Arora, *Chem. Commun.* **2012**, *48*, 1416–1418.

[7] D. Wang, K. Chen, J. L. Kulp III, P. S. Arora, *J. Am. Chem. Soc.* **2006**, *128*, 9248–9256.

[8] a) L. K. Henchey, K. Swati, D. Ramin, R. N. Chapman, B. Z. Olenyuk, P. S. Arora, *J. Am. Chem. Soc.* **2010**, *132*, 941–943; b) A. Patgiri, K. K. Yadav, P. S. Arora, D. Bar-Sagi, *Nat. Chem. Biol.* **2011**, *7*, 585–587; c) K. Swati, L. Brooke Bullock, L. K. Henchey, D. Ramin, M. Hanah, N. J. Traaseth, B. Z. Olenyuk, P. S. Arora, *Proc. Natl. Acad. Sci. USA* **2013**, *110*, 15602–15607.

[9] a) V. Hack, C. Reuter, R. Opitz, P. Schmieder, M. Beyermann, J.-M. Neudörfl, R. Kühne, H.-G. Schmalz, *Angew. Chem. Int. Ed.* **2013**, *52*, 9539–9543; *Angew. Chem.* **2013**, *125*, 9718–9722; b) J. Fremaux, L. Mauran, K. Pulka-Ziach, B. Kauffmann, B. Odaert, G. Guichard, *Angew. Chem. Int. Ed.* **2015**, *54*, 9816–9820; *Angew. Chem.* **2015**, *127*, 9954–9958.

[10] a) R. N. Chapman, P. S. Arora, *Org. Lett.* **2006**, *8*, 5825–5828; b) A. Patgiri, M. R. Witten, P. S. Arora, *Org. Biomol. Chem.* **2010**, *8*, 1773–1776.

[11] a) R. Aurora, G. D. Rosee, *Protein Sci.* **1998**, *7*, 21–38; b) S. Penel, E. Hughes, A. J. Doig, *J. Mol. Biol.* **1999**, *287*, 127–143.

[12] S. Arttamangkul, J. E. Ishmael, T. F. Murray, D. K. Grandy, G. E. DeLander, B. L. Kieffer, J. V. Aldrich, *J. Med. Chem.* **1997**, *40*, 1211–1218.

[13] A. J. Vernall, P. Cassidy, P. F. Alewood, *Angew. Chem. Int. Ed.* **2009**, *48*, 5675–5678; *Angew. Chem.* **2009**, *121*, 5785–5788.

[14] A. Pardi, M. Billeter, K. Wuthrich, *J. Mol. Biol.* **1984**, *180*, 741–751.

[15] J. Graf, P. H. Nguyen, G. Stock, H. Schwalbe, *J. Am. Chem. Soc.* **2007**, *129*, 1179–1189.

[16] a) F. Jiang, Y.-D. Wu, *J. Am. Chem. Soc.* **2014**, *136*, 9536–9539; b) F. Jiang, C.-Y. Zhou, Y.-D. Wu, *J. Phys. Chem. B* **2014**, *118*, 6983–6998.

[17] C.-Y. Zhou, F. Jiang, Y.-D. Wu, *J. Phys. Chem. B* **2015**, *119*, 1035–1047.

[18] J. Wang, R. M. Wolf, J. W. Caldwell, P. A. Kollman, D. A. Case, *J. Comput. Chem.* **2004**, *25*, 1157–1174.

[19] C. I. Bayly, P. Cieplak, W. Cornell, P. A. Kollman, *J. Phys. Chem.* **1993**, *97*, 10269–10280.

[20] H. Geng, F. Jiang, Y. D. Wu, *J. Phys. Chem. Lett.* **2016**, *7*, 1805–1810.

[21] X. Daura, K. Gademann, B. Jaun, D. Seebach, W. F. van Gunsteren, A. E. Mark, *Angew. Chem. Int. Ed.* **1999**, *38*, 236–240; *Angew. Chem.* **1999**, *111*, 249–253.

[22] D. Wang, K. Chen, G. Dimartino, P. S. Arora, *Org. Biomol. Chem.* **2006**, *4*, 4074 – 4081.

[23] a) F. Rastinejad, P. Huang, V. Chandra, S. Khorasanizadeh, *J. Mol. Endocrinol.* **2013**, *51*, T1 – T21; b) B. J. Deroo, K. S. Korach, *J. Clin. Invest.* **2006**, *116*, 561 – 570.

[24] a) J. D. Norris, L. A. Paige, D. J. Christensen, C. Y. Chang, M. R. Huacani, D. Fan, P. T. Hamilton, D. M. Fowlkes, D. P. McDonnell, *Science* **1999**, *285*, 744 – 746; b) A. M. Leduc, J. O. Trent, J. L. Wittliff, K. S. Bramlett, S. L. Briggs, N. Y. Chirgadze, Y. Wang, T. P. Burris, A. F. Spatola, *Proc. Natl. Acad. Sci. USA* **2003**, *100*, 11273 – 11278; c) A. K. Galande, K. S. Bramlett, T. P. Burris, J. L. Wittliff, A. F. Spatola, *J. Pept. Res.* **2004**, *63*, 297 – 302; d) A. K. Galande, K. S. Bramlett, J. O. Trent, T. P. Burris, J. L. Wittliff, A. F. Spatola, *ChemBioChem* **2005**, *6*, 1991 – 1998; e) T. R. Geistlinger, R. K. Guy, *J. Am. Chem. Soc.* **2003**, *125*, 6852 – 6853; f) T. R. Geistlinger, A. C. McReynolds, R. K. Guy, *Chem. Biol.* **2004**, *11*, 273 – 281; g) C. Phillips, L. R. Roberts, M. Schade, R. Bazin, A. Bent, N. L. Davies, R. Moore, A. D. Pannifer, A. R. Pickford, S. H. Prior, C. M. Read, A. Scott, D. G. Brown, B. Xu, S. L. Irving, *J. Am. Chem. Soc.* **2011**, *133*, 9696 – 9699; h) S. Fuchs, H. D. Nguyen, T. T. Phan, M. F. Burton, L. Nieto, I. J. de Vries-van Leeuwen, A. Schmidt, M. Goodarzifard, S. M. Agten, R. Rose, C. Ottmann, L. G. Milroy, L. Brunsveld, *J. Am. Chem. Soc.* **2013**, *135*, 4364 – 4371; i) L.-G. Milroy, L. Brunsveld, *Future Med. Chem.* **2013**, *5*, 2175 – 2183.

[25] L. D. Walensky, A. L. Kung, I. Escher, T. J. Malia, S. Barbuto, R. D. Wright, G. Wagner, G. L. Verdine, S. J. Korsmeyer, *Science* **2004**, *305*, 1466 – 1470.

[26] B. Vaz, S. Mocklinghoff, S. Folkertsma, S. Lusher, J. de Vlieg, L. Brunsveld, *Chem. Commun.* **2009**, 5377 – 5379.

[27] J. L. Vanhooke, M. M. Benning, C. B. Bauer, J. W. Pike, H. F. DeLuca, *Biochemistry* **2004**, *43*, 4101 – 4110.

[28] a) S. Bolte, F. P. Cordelieres, *J. Microsc.* **2006**, *224*, 213 – 232; b) P. Venco, M. Bonora, C. Giorgi, E. Papaleo, A. Iuso, H. Prokisch, P. Pinton, V. Tiranti, *Front. Genet.* **2015**, *6*, 185.

[29] a) M. Carraz, W. Zwart, T. Phan, R. Michalides, L. Brunsveld, *Chem. Biol.* **2009**, *16*, 702 – 711; b) R. M. Martin, G. Ter-Avetisyan, H. D. Herce, A. K. Ludwig, G. Lattig-Tunnemann, M. C. Cardoso, *Nucleus* **2015**, *6*, 314 – 325; c) T. Nagakubo, Y. Demizu, Y. Kanda, T. Misawa, T. Shoda, K. Okuhira, Y. Sekino, M. Naito, M. Kurihara, *Bioconjugate Chem.* **2014**, *25*, 1921 – 1924.

[30] a) K. Tints, M. Prink, T. Neuman, K. Palm, *Int. J. Mol. Sci.* **2014**, *15*, 5680 – 5698; b) Y. Demizu, T. Misawa, T. Nagakubo, Y. Kanda, K. Okuhira, Y. Sekino, M. Naito, M. Kurihara, *Bioorg. Med. Chem.* **2015**, *23*, 4132.Bumple250

Received: July 14, 2016
Published online: August 30, 2016

